

# Thin film shape memory composites

Bernhard Winzek, Tobias Sterzl, Holger Rumpf, Nikolai Botkin, Eckhard Quandt  
center of advanced european studies and research (caesar), Bonn, Germany

## Introduction

Thin film shape memory alloys have been investigated since 1990, when first reports about the deposition of TiNi films by magnetron sputtering were published [1,2]. Since then, investigations have been made to clarify the influence of the sputtering conditions to the stoichiometry of the deposited films [3], the growth of precipitates [4,5], and the thermo-elastic behavior of the TiNi films [6,7].

After the realization of binary TiNi films, several reports described the fabrication of ternary SMA films and their properties. Chang [8] and Hashinaga et al. [9] investigated the properties of Ti(Ni,Cu) films. Subsequently, Ti(Ni,Pd) [10] and (Ti,Hf)Ni [11] films were realized by magnetron sputtering. It was found, that the essential properties of the bulk materials, e.g. the reduction of the hysteresis by the substitution of Ni with Cu, or the enhancement of the transformation temperatures by the substitution of Ni with Pd or Ti with Hf, could be confirmed in thin SMA layers. It was also found, that the grain size, the purity as well as the density and size of precipitates affect significantly the shape memory properties of the deposited films.

Within the last years, several attempts have been made to use the advantageous properties of shape memory thin films in robotics, microfluidic as well as in pneumatic applications. Kuribayashi et al. proposed to use intrinsic stresses by aligned precipitates in the SMA films to obtain a two-way shape memory effect and to use this method for the fabrication of a microgripper [12]. In further approaches, external stresses were applied to the SMA films to generate a two-way behavior. By means of this method, Bernard et al. performed a micropump [13] whereas Johnson et al. [14] as well as Kohl et al. [15] fabricated microvalves. However, a special way to apply external stresses to a SMA film is the creation of a composite consisting of the SMA film and a substrate with a differing thermal expansion coefficient [16-18]. By means of heat treatments, high film stresses can be generated within the SMA film resulting in the required two-way behavior of the total composite. The properties and the feasibility of such composites are the main topics of the following sections. Furthermore, SMA composites with bistable properties and special SMA composites exhibiting wave-like behavior are presented. Finally some potential applications are addressed.

## 1. Functional principle of thin film substrate composites

In contrast to free-standing films, SMA films deposited on metallic foils or on Si wafers are not able to provide strain changes of about 8 percent, since the substrate material cannot stand these large strains without plastic deformation. However, many substrate materials stand large stresses. Mo, for example, has a yield stress of about 600 MPa. This high stress value can be applied to SMA films, if the thermal expansion coefficients of film and substrate differ significantly, the Young's modulus of the substrate is higher than the one of the SMA and the corresponding composites are treated at temperatures above the recrystallization temperature of the SMA. After the heat treatment, upon cooling, the thermally induced stress in the composite increases until the SMA reaches the martensitic start temperature  $M_s$ . As a consequence, the increasing stress in the film substrate composite leads to the bending of the film composite. Upon further cooling, the SMA subsequently undergoes the martensitic transformation. Due to the generation of preferentially oriented martensitic variants upon this transformation, the thermally induced stress in the SMA is reduced significantly and the bending of the composite is reversed. Figure 1 shows the stress-temperature curve of a  $Ti_{52}Ni_{39}Cu_9$  film on a Si substrate after heat treatment at 600°C. The linear part of the curve corresponds to the bimetallic effect and the hysteresis to the shape memory effect. The stress decrease of about 400 MPa due to the martensitic transformation can be regenerated simply by reheating the composite to the austenitic state. The stress which remains in the martensitic state is related to the superelastic plateau stress of the SMA. Therefore, the usable magnitude of the effect is restricted to the stress difference between the yield stress of the austenite of about 600 MPa and the superelastic plateau stress of the SMA of at least 100 MPa. This stress difference is called recoverable stress according to the constrained recovery effect.

Since there are substrate materials with thermal expansion coefficients higher as well as lower

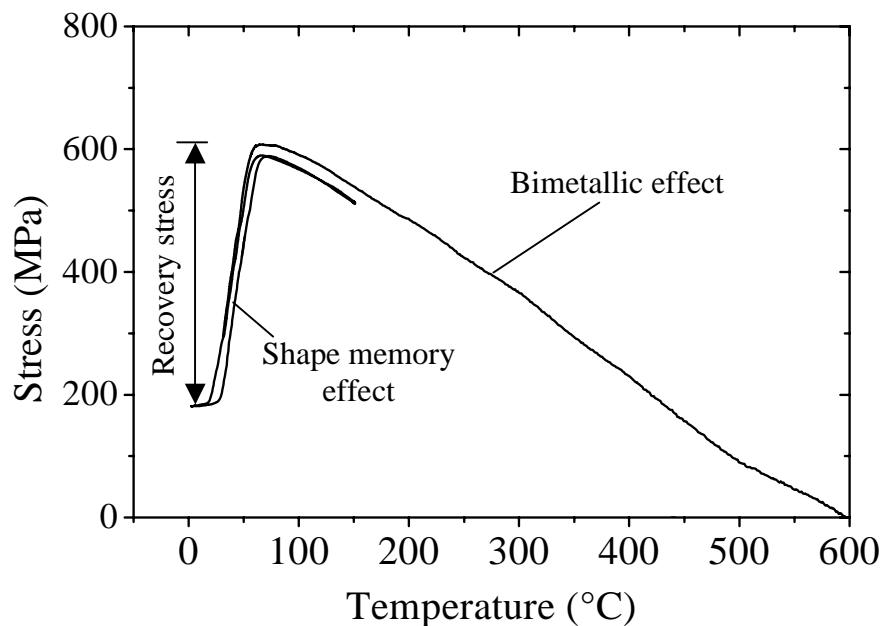


**Figure 1:** Film stress vs. temperature curve of a  $Ti_{52}Ni_{39}Cu_9$  film deposited on a Si substrate after annealing at 600°C for 45 minutes.

**Table 1:** Young's modulus  $Y$ , Poisson number  $\nu$  and expansion coefficients  $\alpha$  at  $100^\circ\text{C}$  of TiNi in the austenitic state, Mo, and  $\text{Fe}_{72}\text{Cr}_{18}\text{Ni}_{10}$ . \* estimated value.

	$Y$ / GPa	$\nu$	$\alpha$ / $\text{K}^{-1}$
TiNi	60-90	0.3*	$11 \cdot 10^{-6}$
Mo	325	0.293	$5.2 \cdot 10^{-6}$
Si [100]	169	0.064	$3.1 \cdot 10^{-6}$
$\text{Fe}_{72}\text{Cr}_{18}\text{Ni}_{10}$	190-210	0.3*	$18 \cdot 10^{-6}$

than those of TiNi-based alloys, it is possible to perform compressive as well as tensile stresses within the SMA films. Table 1 lists the essential thermo-mechanical properties of TiNi as well as the used Mo, Si and steel substrates. Mo and Si substrates were chosen due to their low expansion coefficient in comparison to TiNi.  $\text{Fe}_{72}\text{Cr}_{18}\text{Ni}_{10}$  substrates were selected due to their relatively high expansion coefficient.

## 2. Work output of shape memory composites

The work output of shape memory composites is related to the recovery stress upon the reverse martensitic transformation from martensite to austenite. Since this recovery stress is generated within a temperature range which is narrow in comparison to the thermally induced stress of the corresponding bimetallic effect (Figure 1), the work output of SMA composites is significantly higher than the one of bimetals. In the case of the  $\text{Ti}_{52}\text{Ni}_{39}\text{Cu}_9/\text{Si}$  composite in Figure 1 the SMA effect is even ten times larger. The photos in Figure 2 of a TiNiCu/Mo composite with an overall thickness of  $35 \mu\text{m}$  show, that the thin composite is able to lift about 100 times its own weight.

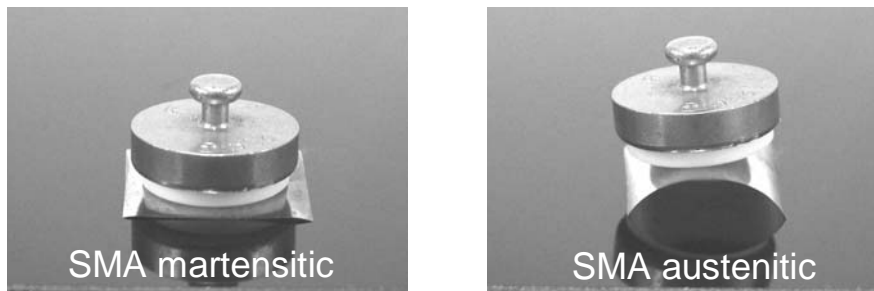


**Figure 2:** Photos of a TiNiCu/Mo composite in the martensitic and austenitic state, respectively. The thickness of the TiNiCu film is  $10 \mu\text{m}$  and the thickness of the Mo  $25 \mu\text{m}$ .

To get the highest possible work output, the thickness of the SMA film has to be adjusted to the mechanical properties of the substrate. Rigid substrates are able to apply high stresses to the SMA films, however, they deliver no work output. Soft substrates are not able to apply stresses to the SMA films resulting again in minimum work output. In the case of Mo substrates, calculations showed, that a thickness ratio of film to substrate of about 0.5 is optimum for high work output. The SMA composite in Figure 2 exhibits a work output of  $0.1 \text{ J/cm}^3$  (Volume includes substrate).

Beside the thicknesses of film and substrate, the design of the composite has also great influence on the work output of a thin film actuator. FEM calculations of the elastic energy density in bimetallic composites reveal, that the lateral dimensions affect significantly the curvature of the corresponding composite. While in composites with a low thickness ratio of film and substrate, the bending of the actuator is two-dimensional like the surface of a sphere, the composites with a film thickness comparable to the substrate thickness bend only in one dimension. Energy minimum is reached when the axis of the curvature is as long as possible, which means, in the case of a rectangular shaped composite, it is aligned along the diagonal. The diagram in Figure 3 shows the elastic energy density vs. the ratio of the dimensions of a rectangular shaped composite for three different boundary conditions. The straight line indicates the case, where the curvature of the composite is completely suppressed. In the second case, the curvature along the edge  $a$  is suppressed (dashed line) and in the third case, the composite can bend freely (dotted line). The maximum work output of a thin film actuator is half the energy difference between the curves of a bended composite (dashed or dotted line) and the curve of the flat composite (straight line at  $0.375 \text{ J/cm}^3$ ). The curvature which is found by experiment is always the one which corresponds to the lowest elastic energy and which therefore provides the highest work output. It can be concluded, that the maximum work output can be provided from composites, that are not restricted in their bending behavior, which means that they can bend freely. Since in general, there is often a small anisotropy in the elastic properties of a metal foil, especially when the foil is cold rolled, the curvature along the short edge of rectangular shaped composites can be found in most experiments.

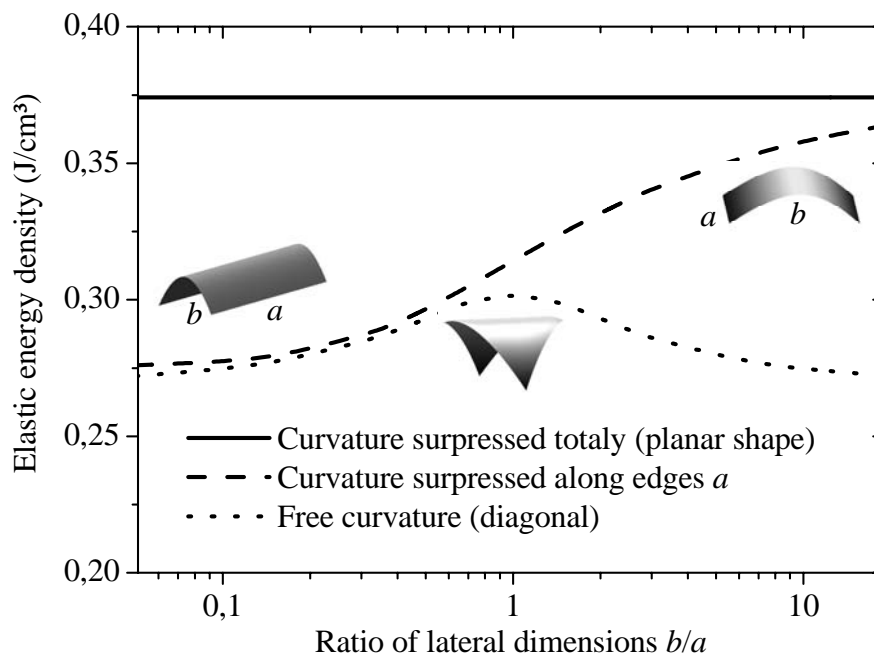


**Figure 3:** Calculated elastic energy density vs. ratio of lateral dimensions of TiNi/Mo composites at  $100^\circ\text{C}$  after heat treatment at  $600^\circ\text{C}$ . The composites are forced to different boundary conditions.

In the case of electrical switches with thin film SMA composites being the active element, restricted boundary conditions have to be considered. In general, the composites have to be detached on substrates, the curvature should be clearly defined and the electrical contacts should be realized tangentially. For this purpose, S-shaped actuators by patterned composites with an alternating deposition sequence are proposed, since in this case, the deflection of the actuators is high and the electric contact can be realized tangentially. Figure 4 shows the drawing of such an actuator. At the lower part of the actuator, the SMA film is deposited on top and at the upper part, the SMA film is on the bottom side of a metallic interlayer (e.g. Mo). Due to the alternating curvature of the actuator, the bending around the x-axis is suppressed and therefore the curvature in both SMA components is forced around the y-axis.

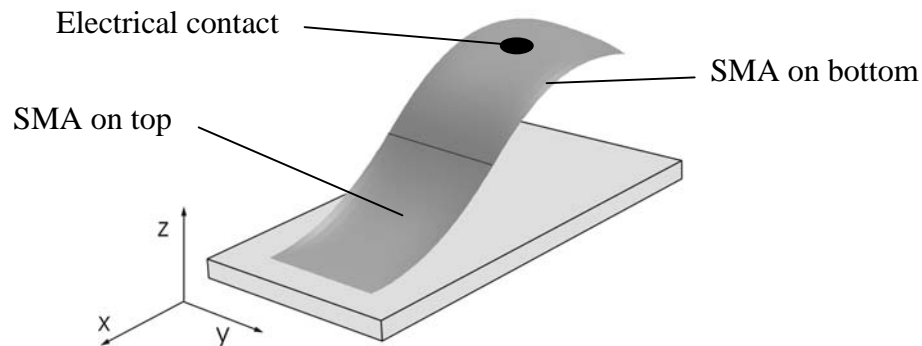


**Figure 4:** Calculated shape of a TiNi/Mo actuator at 100°C (austenite) after heat treatment at 600°C. In the martensitic state the actuator is planar.

### 3. Shape memory alloys for thin film composites

For the adjustment of the transformation temperatures and hysteresis properties, respectively, several different SMAs can be used. Mostly, TiNi-based alloys are preferred, due to their low sensitivity to aggressive media. Binary TiNi alloys provide different martensitic transformations: the two-step B2→R-phase→B19' transformation and the direct B2→B19' transformation. Usually, the B2→R-phase transformation is preferred for actuator applications, since it exhibits a very narrow hysteresis and since it is less sensitive to deviations in stoichiometry and lattice defects [19]. It can be realized either in off-stoichiometric alloys, where precipitates hinder the transformation into the monoclinic B19' phase or by dislocation networks in the case of stoichiometric alloys. However, in contrast to the B2→R-phase transformation the B2→B19'-transformation delivers a significantly higher magnitude of effect. Figure 5 shows the stress vs. temperature curve of a binary TiNi film on a Mo substrate. The step-wise change in the film stress corresponds to the B2→R-phase→B19' transformation. Upon heating, the curve indicates, that the TiNi film transforms directly into the B2 phase. Figure 6 reveals that the B2→R-phase transformation can be used separately benefiting from the narrow hysteresis and a recovery stress of 100 MPa. Stable transformation temperatures combined with a large magnitude of effect can be realized using Ti(Ni,Cu) alloys. The stress temperature curve of a Ti(Ni,Cu)/Si composite is depicted

in Figure 1. The hysteresis width is about 10 K and the recovery stress is about 400 MPa. A similar magnitude of recovery stress has been found in (Ti,Hf)Ni-alloys. In these alloys, the transformation temperatures increase with increasing Hf content up to 500°C, while the hysteresis width is comparable to the one of binary TiNi. Figure 7 shows the stress-temperature curve of a  $\text{Ti}_{46}\text{Hf}_6\text{Ni}_{48}$  film on Mo.

In some cases, elevated transformation temperatures are required combined with a hysteresis width narrower than the one of (Ti,Hf)Ni alloys. For this purpose, thin film composites with Ti(Ni,Pd) films on Mo substrates were fabricated and characterized. By substitution of Ni with Pd the transformation temperatures can be elevated up to 500°C, however with a hysteresis width of about 30 K. The stress-temperature curve of a  $\text{Ti}_{54}\text{Ni}_{26}\text{Pd}_{30}$  film is depicted in figure 8 revealing that the shape memory effect occurs above 200°C, which is convenient for applications with floating environmental temperatures and applications which require higher cooling rates.

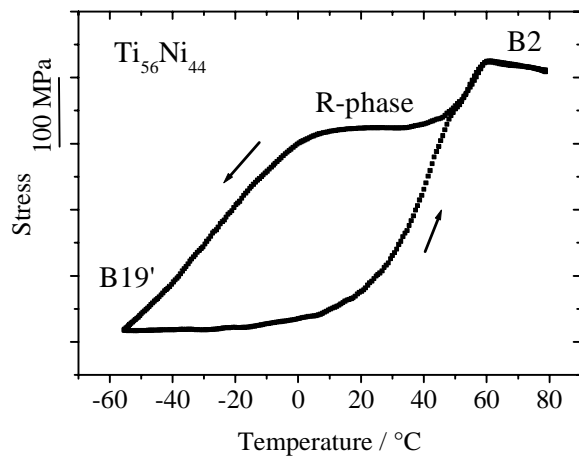


**Figure 5:** Stress-temperature curve of a  $1,4 \mu\text{m}$  TiNi-film on a  $46 \mu\text{m}$  Mo substrate. Temperature cycled between  $-55^\circ\text{C}$  and  $80^\circ\text{C}$ .

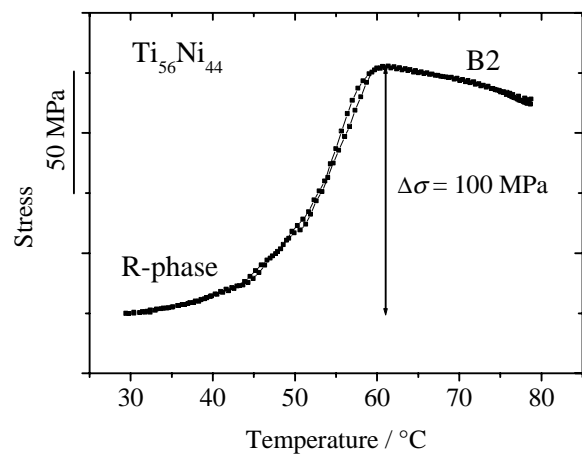


**Figure 6:** Stress-temperature curve of a  $1,4 \mu\text{m}$  TiNi-film on a  $46 \mu\text{m}$  Mo substrate. Temperature cycled between  $30^\circ\text{C}$  and  $80^\circ\text{C}$ .

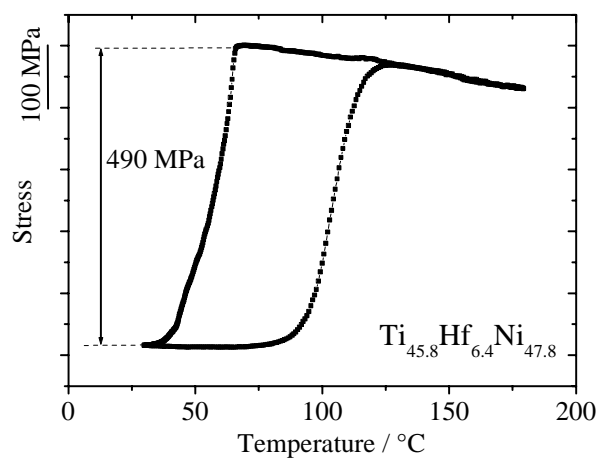


**Figure 7:** Stress-temperature curve of a  $2 \mu\text{m}$   $\text{Ti}_{46}\text{Hf}_6\text{Ni}_{48}$  film on a  $100 \mu\text{m}$  Mo substrate.

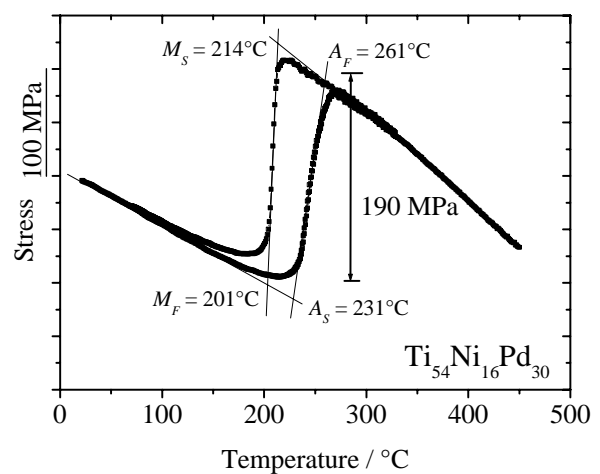


**Figure 8:** Stress-temperature curve of a  $4,4 \mu\text{m}$  Ti(Ni,Pd)-film on a  $46 \mu\text{m}$  Mo substrate.

With increasing transformation temperatures the magnitude of effect, meaning the recovery stress, decreases, since the recovery stress is limited by the thermally induced stress which can be generated between the recrystallization temperature and martensite start temperature. The brittleness of the (Ti,Hf)Ni and Ti(Ni,Pd) films is neglectable, as long as the SMA films are deposited onto ductile substrates. Therefore, a large variety of SMA films can be used in composite actuators.

#### 4. Adjustment of the curvature

The curvature of SMA composites consisting of two layers, the SMA film and the substrate, is defined by the high stress state austenite and the relaxed martensite state of the SMA film. In the case of an austenitic SMA and a substrate with a lower expansion coefficient than the SMA, the SMA film is under tensile stress and in the case of a substrate with a higher thermal expansion coefficient, the SMA film is under compressive stress. According to this different stress states, the curvature of the austenitic SMA composite can be selected by the choice of the substrate material.

In some applications, however, it is useful to have a bended composite in the low temperature state and a flat composite in the high-temperature state. Or sometimes it might be convenient to switch the curvature from concave to convex or vice versa by means of the martensitic transformation. For this purpose, a three-layer system with a SMA layer and two additional layers is recommended, as demonstrated first by Kim et al. [20].

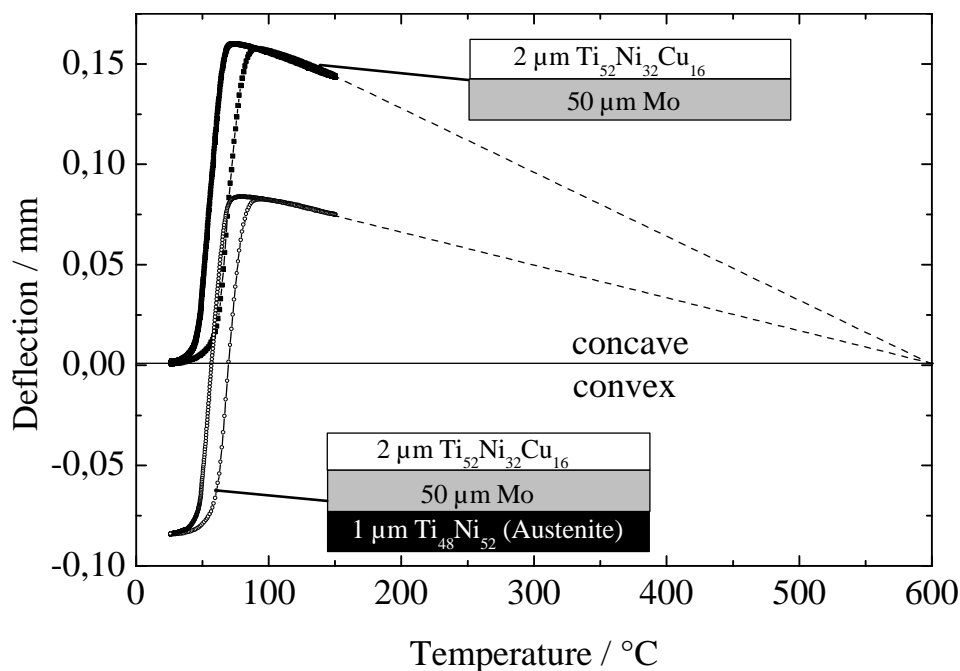


**Figure 9:** Deflection vs. temperature of two different SMA composites. By means of an additional Ni-rich TiNi layer, the offset of the cantilever was shifted to the convex regime.

Figure 9 shows the deflection-temperature measurements of two different cantilevers. One deflection-temperature curve results from a TiNiCu/Si composite and the second one from a TiNiCu/Si/TiNi system, whereby the TiNi layer is Ni-rich exhibiting no shape memory effect. By means of this additional metallic layer, the bimetallic effect of the SMA layer can be reduced and the curvature of the SMA composite can be adjusted. Since the deflection of the cantilever according to the bimetallic effect was reduced by about 50 %, the curvature of the total composite can be switched from concave to convex and vice versa. If the passive Ni-rich TiNi-layer has the same thickness as the active TiNiCu layer, the bimetallic effect can be completely compensated [20].

## 5. Bistable shape memory composites

If shape memory alloys and thermo-elastic polymers are combined, composites can be created which show a bistable behavior. The essential precondition for the bistability is that the Young's modulus or the shear modulus of the polymer decreases significantly within the hysteresis of the shape memory alloy. Figure 10 shows the superposition of the hysteresis of a SMA and the Young's modulus of a thermo-elastic polymer, according to this precondition. If both materials are heated to a temperature above the austenite finish temperature  $A_f$ , the polymer is already in a soft state before the SMA reaches the austenitic state. In the case of a shape-memory film on a metallic substrate, the austenitic state is correlated with the bended state of the SMA-composite. Since the polymer is soft, the total SMA-substrate-polymer composite is bended. Upon cooling the polymer becomes hard before the SMA is martensitic. Therefore, the complete composite remains bended also in the low temperature state. If the

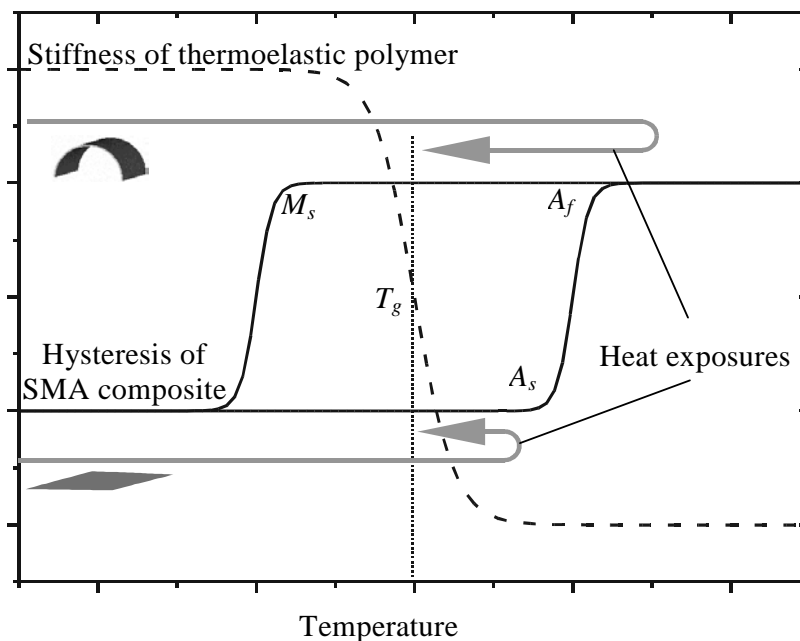


**Figure 10:** Young's modulus vs. temperature curve of a thermoelastic polymer and transformation hysteresis of a SMA composite. Arrows indicate the heat exposures to change the curvature of the actuator.

materials are heated to a temperature between the glass transition temperature of the polymer  $T_g$  and the austenite start temperature  $A_s$ , the polymer becomes soft and releases the SMA. The SMA is still martensitic and therefore corresponds to the flat shape of the SMA-composite. Upon cooling, the polymer fixes the flat shape of the martensitic SMA. As a consequence, the composite can be switched by means of two different heat exposures from the flat to the bended shape and vice versa. Energy is only necessary for the switching process. Hence, the energy consumption of the SMA can be significantly reduced and an excessive thermal load of the adjacent structures can be avoided.

For the realization of the bistable composite it is recommended to use a (Ti,Hf)Ni alloy due to its broad hysteresis. A suitable polymer is PMMA since it shows a large decay of the Young's modulus at about  $100^\circ\text{C}$ . Figure 11a shows the cross section of a SMA film substrate composite covered by a polymer. The different bending states of a ( $10\mu\text{m Ti}_{46}\text{Hf}_6\text{Ni}_{48}$ )/( $25\mu\text{m Mo}$ ) composite enclosed in a Lucryl<sup>®</sup> polymer are shown in Figure 11b and 11c. The photos were taken at room temperature after heat exposure to  $90^\circ\text{C}$  (Figure 11b) and after heat exposure to  $120^\circ\text{C}$  (Figure 11c). The bending states can be switched by the different heat exposures. The process is reversible.

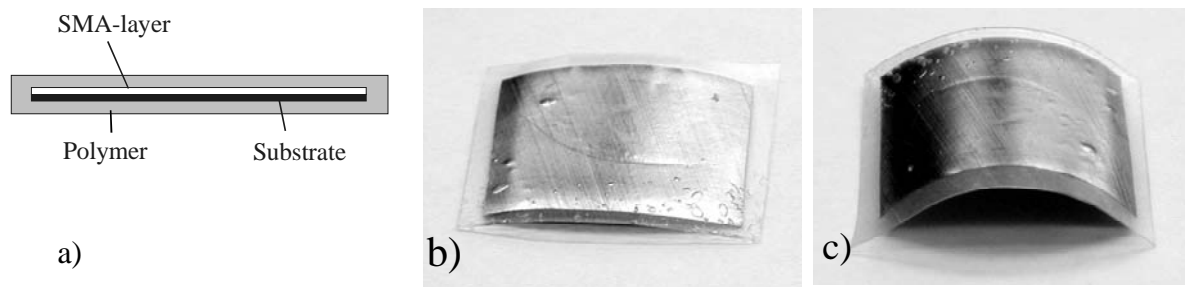


**Figure 11:** Bistable composite  $\text{Ti}_{46}\text{Hf}_6\text{Ni}_{48}/\text{Mo}$  covered by Lucryl<sup>®</sup> at room temperature. a) Cross section, b) photo after heat exposure to  $90^\circ\text{C}$  and c) photo after heat exposure to  $120^\circ\text{C}$ .

## 6. Phase-coupled shape memory composites

Shape memory actuators are necessarily coupled to adjacent actuators, if there is any heat flow between them. In this case, usually, the transformation sequence is obvious. Upon heating, the actuator with the lower transformation temperature and upon cooling the one with the higher transformation temperature transforms first. Since each SMA in general provides a distinct hysteresis, it is possible to generate another transformation sequence, whereby one of the two SMAs always starts to transform at first, upon heating as well as upon cooling. This special transformation sequence can be achieved, if one shape memory alloy A has its narrow hysteresis embedded within the broad hysteresis of an alloy B (Figure 12). The overall transformation sequence is  $A\uparrow B\uparrow A\downarrow B\downarrow$ , whereby the arrow upwards  $\uparrow$  denotes the reverse martensitic transformation from martensite to austenite and the arrow downwards  $\downarrow$  indicates the martensitic transformation from austenite to martensite.

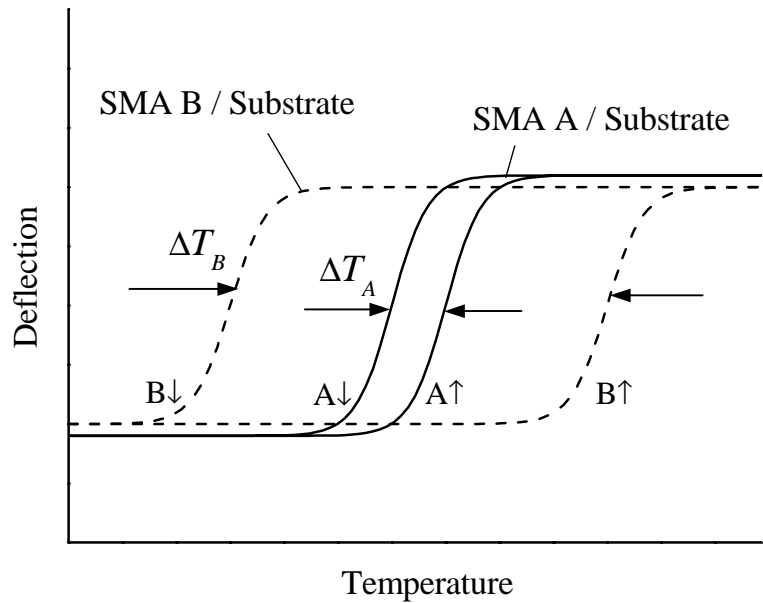


**Figure 12:** Schematic deflection vs. temperature curves of cantilevers containing either a SMA A or a SMA B (dashed line) with different hysteresis widths. The arrow downwards ↓ depicts the martensitic transformation and the arrow upwards ↑ the reverse transformation.

The combination of the SMA alloys Ti(Ni,Cu) and (Ti,Hf)Ni allows the realization of this concept. Ti(Ni,Cu) is chosen due to its low hysteresis width and (Ti,Hf)Ni is selected since this alloy provides a broad hysteresis width and adjustable transformation temperatures. Figure 13 shows the superposition of the deflection measurements of a  $\text{Ti}_{52}\text{Ni}_{34}\text{Cu}_{14}/\text{Mo}$  and a  $\text{Ti}_{47}\text{Hf}_{11}\text{Ni}_{42}/\text{Mo}$  composite. It can be seen that both deflection vs. temperature curves fit very well to the required conditions. The hysteresis of the  $\text{Ti}_{52}\text{Ni}_{34}\text{Cu}_{14}/\text{Mo}$  composite is adjusted within the hysteresis of the  $\text{Ti}_{47}\text{Hf}_{11}\text{Ni}_{42}/\text{Mo}$  composite and the magnitude of effect of both composites is rather similar.

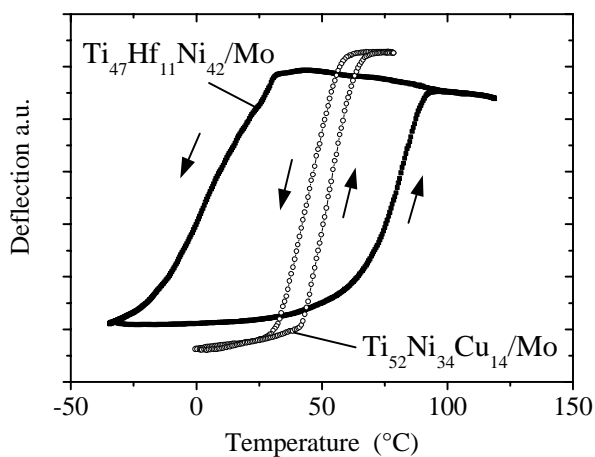


**Figure 13:** Deflection-temperature measurements of SMA-film-substrate cantilevers.

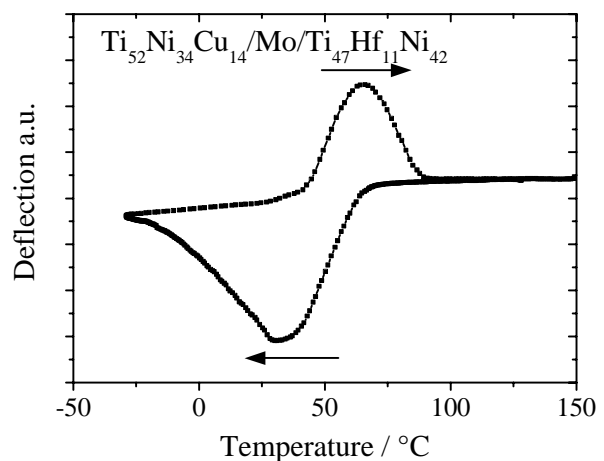


**Figure 14:** Deflection-temperature measurement of a  $\text{Ti}_{52}\text{Ni}_{34}\text{Cu}_{14}/\text{Mo}/\text{Ti}_{47}\text{Hf}_{11}\text{Ni}_{42}$  cantilever.

If both SMAs work in opposite directions as it can be realized easily in thin film composites by depositing the SMAs on opposite sides of the substrate, the path of deflection upon heating is completely different from the path upon cooling as illustrated in Figure 14. Upon heating the  $\text{Ti}_{52}\text{Ni}_{34}\text{Cu}_{14}/\text{Mo}/\text{Ti}_{47}\text{Hf}_{11}\text{Ni}_{42}$  composite bends upwards and upon cooling downwards. If both SMAs are martensitic, they are soft and not able to pull the substrate in their direction resulting in zero deflection. If both SMAs are austenitic they pull with the same force in opposite directions which also leads to zero deflection of the actuator. The difference between the heating and the cooling stages arises from the fact, that upon heating there is a temperature interval in which SMA A is austenitic and SMA B is martensitic. Upon cooling the situation is vice versa.

To demonstrate this special transformation sequence of the combination of  $\text{Ti}_{52}\text{Ni}_{34}\text{Cu}_{14}$  and  $\text{Ti}_{47}\text{Ni}_{11}\text{Hf}_{42}$ , a special composite was constructed according to the drawing in Figure 15. The photos in Figure 16 show the corresponding motion sequence of this composite. It starts with the flat shape at  $-20^\circ\text{C}$  where both SMAs are in the martensitic state (Figure 16a). Upon heating, first the  $\text{Ti}_{52}\text{Ni}_{34}\text{Cu}_{14}$  films lift the edges (Figure 16b), before the  $\text{Ti}_{47}\text{Ni}_{11}\text{Hf}_{42}$  films raise the center part by turning down (Figure 16c). Upon cooling, first the  $\text{Ti}_{52}\text{Ni}_{34}\text{Cu}_{14}$  film relaxes, which leads to an elevated height (Figure 16e). Finally, at about  $-20^\circ\text{C}$ , the martensitic transformation results in a flat shape of the total actuator (Figure 16f).

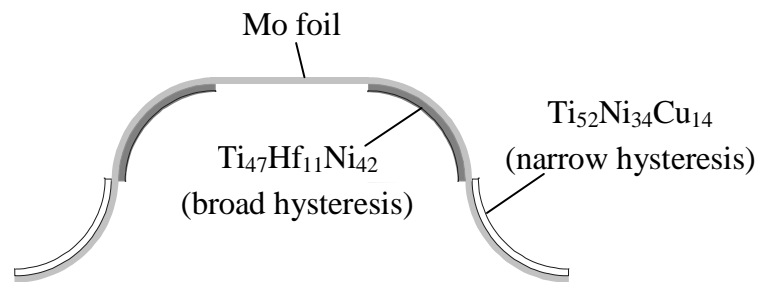


**Figure 15:** Cross-section of a SMA composite to demonstrate the transformation sequence ABAB.

The above described actuator which consists of both SMAs on opposite sides of the substrate is suitable to illustrate and measure the motion capability and smartness of the material combination, but its design has to be advanced to work as a motion principle of a robot. For this purpose, the different SMAs have to be patterned as illustrated in Figure 17, where the cross-section of a robot leg is drawn as a superposition of the four different stages of a complete motion cycle. The SMA B with the broad hysteresis is placed at the upper part and SMA A at the lower part of the actuator. Every motion step corresponds to a different combination of austenite and martensite of the two SMAs. The stages are marked by the four phases  $\varphi_1$ ,  $\varphi_2$ ,  $\varphi_3$  and  $\varphi_4$ . In the beginning ( $\varphi_1$ ), both alloys are martensitic and the leg is straight. According to the special overlap of the hysteresis (see Figure 12), SMA A starts with the transformation ( $\varphi_2$ ). The phases  $\varphi_3$  and  $\varphi_4$  are required to pull the leg back to its initial position while other legs have to carry the weight of the robot. It is essential, that a single heat pulse can generate a complete motion cycle including the push off ( $\varphi_4 \rightarrow \varphi_1 \rightarrow \varphi_2$ ) and the initialization step ( $\varphi_2 \rightarrow \varphi_3 \rightarrow \varphi_4$ ).

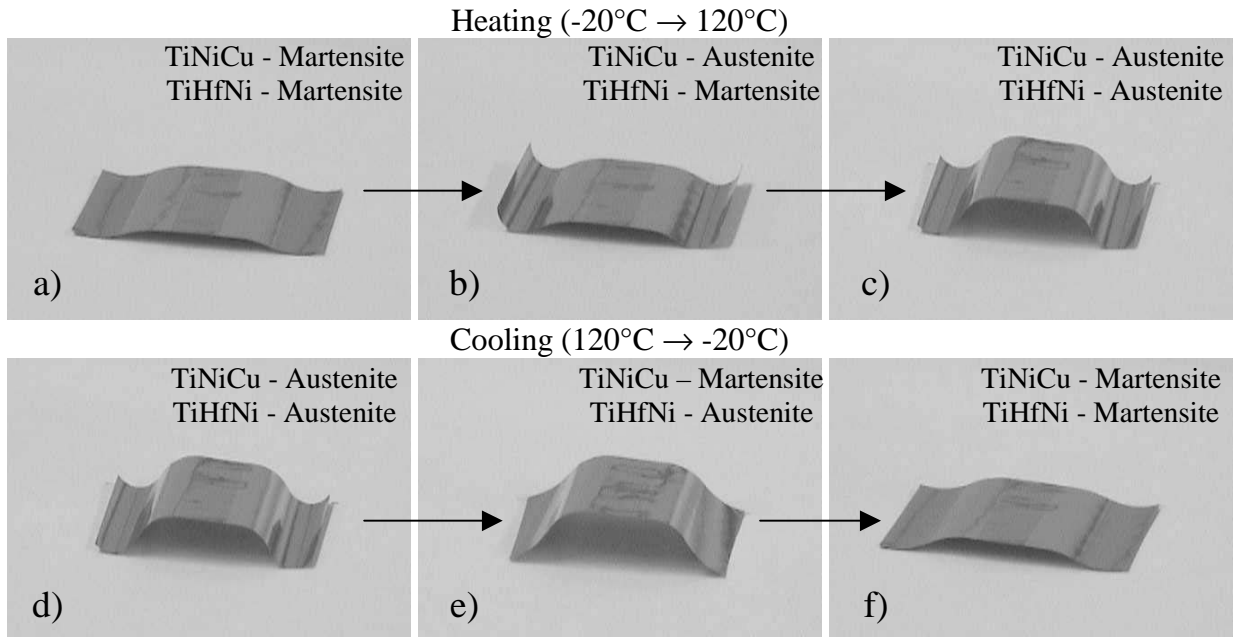


**Figure 16:** Bending states of a Mo foil coated with  $\text{Ti}_{52}\text{Ni}_{34}\text{Cu}_{14}$  and  $\text{Ti}_{47}\text{Ni}_{11}\text{Hf}_{42}$  films according to the drawing in Figure 15 upon heating and cooling.

It was shown in chapter 4, that by means of the additional deposition of metallic layers onto SMA composites, the initial curvature of the actuators can be adjusted. Therefore, the superposition of the shape memory effect and an additional bimetallic effect allows the fabrication of actuators which are plane in the austenitic state and curved in the martensitic state. Considering this variety of actuator states, hence, it is possible to create all four different actuator shapes in Figure 17 with SMA composites that are completely martensitic. As a consequence, a robot can be constructed whereby the complete robot is operated with a single heat pulse causing the phase-shifted motion of all legs.

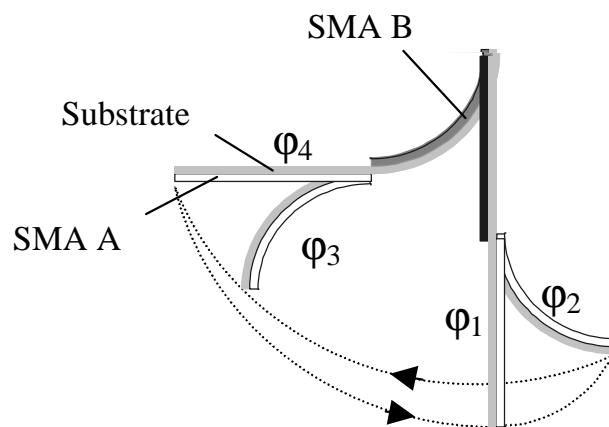


**Figure 17:** Superposition of the cross-section of a robot leg at different phases of a motion cycle.

## **7. Potential applications**

In general, shape memory composites have several advantages over bimetals and can therefore replace bimetals in many applications. SMA composite actuators provide a higher work output than bimetals and show a step-like characteristic in their motion behavior, which is required for switches. Snap elements with bimetals provide also hysteretic motion and the step-like characteristic. Snap elements, however, are difficult to realize in microsystems due to their complex boundary conditions. On the contrary, SMA composites can be scaled down to a few micrometers with less restrictions to the boundary conditions.

### **Bistable microgrippers**

SMA thin film composites are already in use in microgrippers. Microgrippers made from micromachined Si with TiNiCu-films to open the grippers are fabricated at the Lawrence Livermore National Laboratory, CA [21]. A bistable gripper containing TiHfNi and polymer layers is under development at caesar, Bonn, Germany.

### **Valves and pumps for microfluidic or pneumatic applications.**

Different valves and pumps have been fabricated using thin films which base on TiNi [13-15]. However, the large forces of SMA composites still have not been introduced to applications in microfluidics or pneumatics. Particularly, the bistable composites are suitable for the use in valves, where the open and close state has to be hold for a long time without permanent energy consumption. Furthermore, the phase-coupled SMA actuators can be integrated in peristaltic pumps since they exhibit inherent wave-like behavior.

### **Microrobots**

The wave-like behavior of phase-coupled SMA composites is also advantageous for walking or swimming robots. The inherent motion capability of the actuators helps to avoid supplementary on-board electronics which is usually required to control separate actuator components. Large motion steps can be realized in the case of spider-like robots where the joints of the legs are replaced by SMA composites. The legs of the robots can even walk without power supply, if the environmental temperature changes significantly, as it has to be considered in space robotics.

### **Adjustable capacitors**

In high frequency technology there is a strong need for electronic components that allow the adjustment of the transponder frequency. For this purpose, adjustable capacitors with SMA composites can be designed. The capacitance of such a plate like capacitor can be adjusted by SMA actuators which can move in thermoplastic dielectric above its melting point. If the actuator reaches the final position, the thermoplastic dielectric hardens before the SMA actuators become martensitic.

## Adaptive surfaces

SMA composites can perform a defined surface topography, e.g. in the case of embossed printing. They can also change the friction coefficient of a surface, e.g. the surface of a snake like robot. In both cases the bistability is important for the efficiency of the actuator system.

## 8. Conclusions

The functional principle of SMA composites was described and actuators were shown to demonstrate their motion capability. The actuators can be designed for a size from several micrometers to lateral dimensions in the order of centimeters which makes them an important tool for precision mechanics and micromechanics. The SMA composites can be driven by Joule's heat, by induction heating or by a change of the environmental temperature.

Bistable shape memory composites reduce the energy consumption and prevent heating of the environment, since the deflected high temperature state does not require permanent heat supply. This makes these bistable composites especially attractive for applications as microvalves, microswitches microgrippers and adjustable capacitors, which are currently under development.

A particular combination of SMAs with broad and narrow hysteresis provides a special transformation sequence required for actuators with wave-like behavior. It allows the integration of the smartness necessary for a defined motion sequence into the material of the actuator and therefore helps to simplify robot systems. Potential applications of the phase-coupled SMA actuators are walking robots for the exploration of dangerous or unknown territory, particularly in space robotics. Furthermore, the wave-like behavior can be used to drive inchworm or snake-like robots and swimming robots. It has also a high potential for peristaltic pumps. If a wheeled platform is required, the wave-like behavior can be transformed to the wheels by means of a crank shaft.

## References

- [1] J.A. Walker, K.J. Gabriel, M. Mehregany, "*Thin-film processing of TiNi shape memory alloy*", Sensors and Actuators, A21-A23 (1990) p. 243-246.
- [2] A.P. Jardine, H. Zhang, L.D. Wasielesky, "*Investigations into the thin-film fabrication of intermetallic NiTi*", Mat. Res. Soc. Symp. Proc. Vol. 187 (1990) p. 181-186.
- [3] M. Bendahan, J.L. Seguin, P. Canet, H. Carchano, "*NiTi shape memory alloy thin films: composition control using optical emission spectroscopy*", Thin Solid Films 283 (1996) p. 61-66.
- [4] F.F. Gong, H.M. Shen, Y.N. Wang, "*Structures and defects induced during annealing of sputtered near-equiatom NiTi shape memory thin films*", Appl. Phys. Lett., Vol. 69, No. 18 (1996) p. 2656-2658.
- [5] S. Kajiwara, K. Ogawa, T. Kikuchi, T. Matsunaga, S. Miyazaki, "*Formation of*

- nanocrystals with an identical orientation in sputter-deposited Ti-Ni thin films*“, Philosophical Magazine Letters, Vol. 74, No. 3 (1996) p. 395-404.
- [6] A. Ishida, A. Takei, M. Sato, S. Miyazaki, “*Stress-strain curves of sputtered thin films of Ti-Ni*”, Thin Solid Films 281-282 (1996) p. 337-339.
- [7] A. Ishida, M. Sato, S. Miyazaki, “*Mechanical properties of Ti-Ni shape memory thin films formed by sputtering*”, Materials Science and Engineering A273-275 (1999) p. 754-757.
- [8] L. Chang, C. Hu-Simpson, D.S. Grummon, W. Pratt, R. Loloee, “*Structure and Phase Transformations in Thermoelastic Ni<sub>1-x</sub>TiCu<sub>x</sub> Thin Films Prepared by DC-Magnetron Sputtering*”, Mat. Res. Soc. Symp. Proc., Vol. 187 (1990) p. 137-142.
- [9] T. Hashinaga, S. Miyazaki, T. Ueki, H. Horikawa, “*Transformation and deformation behavior in sputter-deposited Ti-Ni-Cu thin films*“, Journal de Physique IV, C8, Vol. 5 (1995) p. 689-694.
- [10] E. Quandt, C. Halene, H. Holleck, K. Feit, M. Kohl, P. Schloßmacher, A. Skokan, K.D. Skrobaneck, “*Sputter deposition of TiNi, TiNiPd and TiPd films displaying the two-way shape memory effect*”, Sensors and Actuators A, Vol. 53 (1996) p. 434-439.
- [11] A.D. Johnson, V.V. Martynov, R.S. Minners, “*Sputter deposition of high transition temperature Ti-Ni-Hf alloy thin films*”, Journal de Physique IV, C8, Vol. 5 (1995) p. 783-787.
- [12] K. Kuribayashi, T. Taniguchi, “*Micron sized arm using reversible TiNi alloy thin film actuators*”, Mat. Res. Soc. Symp. Proc Vol., Vol. 276 (1992) p. 167-175.
- [13] W.L. Benard, H. Kahn, A.H. Heuer, M.A. Huff, “*A Titanium-Nickel Shape Memory Alloy Actuated Micropump*“, Transducers '97, Chicago (1997) p. 361-364.
- [14] A.D. Johnson, J.D. Busch, C.A. Ray, C. Sloan, “*Fabrication of silicon-based shape memory alloy micro actuators*”, Mat. Res. Soc. Symp. Proc., Vol. 276 (1992) p. 151-160.
- [15] M. Kohl, D. Dittmann, E. Quandt, B. Winzek “*Thin film shape memory microvalves with adjustable operation temperature*”, Sensors and Actuators 83 (2000) p. 214-219.
- [16] B. Winzek, E. Quandt, H. Holleck, “*Shape memory thin film composites with adjustable transformation temperatures and hysteresis*”, Actuator 98, Bremen (1998) p. 461-464.
- [17] B. Winzek, E. Quandt, “*Shape-memory Ti-Ni-X-films (X = Cu, Pd) under constraint*”, Zeitschrift für Metallkunde Vol. 90, No. 10 (1999) p. 796-802.
- [18] M. Kohl, D. Dittmann, E. Quandt, B. Winzek, “*Thin film shape memory microvalves with adjustable operation temperature*”, Sensors and Actuators 83 (2000) p. 214-219.
- [19] K. Otsuka, “*Introduction to the R-Phase transition*”, Engineering Aspects of Shape Memory Alloys, T.W. Duerig (Hrsg.), Butterworth-Heinemann (1990) p. 36-45.
- [20] T. Kim, Q. Su, M. Wuttig, “*Thermo-mechanical Ni<sub>50</sub>Ti<sub>50</sub>/Si composite thin film switch*”, Mat. Res. Soc. Symp. Proc., Vol. 360 (1995) p. 375-380.
- [21] P. Krulevitch, A.P. Lee, P.B. Ramsey, J.C. Trevino, J. Hamilton, M.A. Northrup, “*Thin film shape memory alloy microactuators*”, Journal of microelectromechanical systems, Vol. 5, No. 4 (1996) p. 270-282.